

Improved IF Estimation of Multi-Component FM Signals Through Iterative Adaptive Missing Data Recovery

Vaishali S. Amin[†], Yimin D. Zhang[†], and Braham Himed[‡]

[†] Department of Electrical and Computer Engineering, Temple University, Philadelphia, PA, 19122, USA

[‡] RF Technology Branch, Air Force Research Laboratory, Dayton, OH, 45433, USA

Abstract—In this paper, we address a challenging problem of accurate instantaneous frequency (IF) estimation of multi-component non-linear frequency modulated (FM) signals with distinct amplitude levels in the presence of missing data samples. In such scenarios, it is often difficult to resolve the weaker signal components. Besides, missing data-induced artifacts spread in the time-frequency (TF) domain, further complicating IF estimation. We propose a method that iteratively performs missing data recovery in the time-lag domain based on the least squares criterion in conjunction with signal-adaptive TF kernels. The proposed technique successfully resolves signal components with distinct amplitude levels, preserves a high resolution of the auto-terms and achieves robust TF distributions by mitigating the undesired effects of cross-terms and artifacts due to missing data samples. The effectiveness of the proposed method is verified through various simulation results.

Index Terms—Instantaneous frequency estimation, missing samples, non-stationary signals, time-frequency distribution.

I. INTRODUCTION

Many practical signals encountered in radar, sonar, wireless communications and biomedical applications are non-stationary frequency modulated (FM) signals that can be characterized by their instantaneous frequencies (IFs) [1]–[3]. In particular, radar target returns are often modeled as multi-component non-linear FM signals. Magnitudes of such signals may significantly differ due to, e.g., different target sizes.

In practice, such signals may be observed with missing data samples. Missing data scenarios could arise due to line-of-sight obstruction, multipath fading, sensor failures, and removal of impulsive noise. When such missing data last for multiple consecutive sampling intervals, the scenario of burst missing samples emerges. Random or group missing data scenarios could also be a result of intentional irregular sampling that is performed to reduce hardware complexity or to meet the constraints posed on sampling schemes in astronomical, meteorological, and satellite based applications, or gapped synthetic aperture to reduce radar resources in high-resolution synthetic aperture radar (SAR) imaging [4]–[8].

Time-frequency distributions (TFDs) facilitate characterization, analysis and processing of such FM signals, and have found wide applications in this direction [2], [9]. Missing data samples introduce artifacts in the respective TFDs. In the case of random missing samples, these artifacts are uniformly spread in the entire time-frequency (TF) region. However, group missing samples cause superimposed sinc-like patterns which are clustered around true IFs in the TF regions and thus, present a more challenging situation for signal detection and analysis [8]. Usually, the weaker signals are greatly affected by the effects of artifacts and noise, making them more difficult to be detected.

The Wigner-Ville distribution (WVD) is considered as the prototype TFD of bi-linear distributions [10], and provides an optimal representation of mono-component linear FM signals. However, it exhibits excessive cross-terms in the case of non-linear FM signals or multi-component FM signals. Reduced interference distributions (RIDs) are the popular form of bi-linear TFDs that aim to mitigate undesired effects of cross-terms and missing data-introduced artifacts using suitable kernel functions [10]–[13]. The adaptive optimal kernel (AOK) [11] is one of the popular choices for signal-dependent TF kernels. While AOK performs well in suppressing the effects of cross-terms and artifacts in the case of random missing samples, its performance deteriorates in the case when missing data appear in groups.

Several sparsity- and TF kernel-based approaches [8], [14]–[18] that consider signal detection and TFD reconstruction in the presence of missing samples have been proposed in recent years. The time-domain missing data recovery for stationary signals was attempted by the missing-data iterative adaptive approach (MIAA) [19] using Capon spectrum estimation [20], [21]. This method was extended for non-stationary signals in [22], with the application of the MIAA on the instantaneous auto-correlation function (IAF), which is stationary with respect to lag τ , at each time instant. However, this method is suitable only for mono-component non-stationary signals. The recently developed missing data iterative sparse reconstruction (MI-SR) approach [8] provides reliable IF estimation of multi-component non-stationary signals by undertaking missing data recovery in the IAF domain with iterative utilization of the orthogonal matching pursuit (OMP) [23].

The aforementioned approaches often face challenges to

The work of V. S. Amin and Y. D. Zhang is supported in part by a subcontract with Matrix Research, Inc. for research sponsored by the Air Force Research Laboratory under contract FA8650-14-D-1722. The work of Y. D. Zhang is also supported in part by a contract with Altamira Technologies Corp. for research sponsored by the Air Force Research Laboratory under Contract FA8650-18-C-1055.

recover weaker signal components, when the signal components have high variation in their relative amplitudes. Such challenges are amplified in the presence of burst missing data samples. Recently-developed sparse reconstruction-based TF analysis techniques [24]–[26] perform relatively well in estimating IFs of non-linear FM signals with distinct amplitude levels of the components and in the presence of group missing samples. However, these methods either rely on the accuracy of the underlying TFDs, are sensitive to frequency quantization errors, require cumbersome manual tuning of the parameters, or suffer from high computational complexity.

The above observations and aforementioned limitations of the existing methods motivated us to consider robust TFDs of randomly thinned FM signals that consist of multiple close components with highly different amplitudes. Similar to MI-SR [8], our proposed Iterative Adaptive Missing Data Recovery (IA-MDR) algorithm also iteratively performs missing data recovery in the IAF domain. However, unlike MI-SR, which was developed based on OMP, the IA-MDR utilizes the MIAA in the IAF domain as in [22]. This is based on our observations that the OMP-based methods generally fail to provide an accurate IF estimation of the weaker signal components in the case when the signal components have distinct amplitude levels [24]. Besides, unlike MI-SR, in which signal adaptive TF kernels could be used to further enhance the reconstruction performance, the use of signal adaptive TF kernels is incorporated in the iterative process itself in the proposed IA-MDR, to improve reconstruction performance.

In IA-MDR, we begin with the WVD as the underlying TFD. The other RIDs could also be used in lieu of the WVD. In each iteration, missing IAF entries are sequentially updated using the weighted least squares criterion [20], [21] for each time instant, and the spectral amplitudes are estimated using the one-dimensional (1-D) Fourier relationship between the IAF and TFD. Missing TF samples are recovered based on the estimated frequencies and their coefficients. Finally, the AOK is applied to the interpolated IAF for further refinement of the obtained TFD and cross-term mitigation. In the proposed IA-MDR approach, spectrum estimation, missing sample recovery and application of TF kernels are iterated for performance improvement. It is noted that, during each iteration, only originally missing entries are updated with the newly estimated values, whereas the entries associated with the observed data samples are unaltered. After the final iteration, the corresponding RID is achieved using a two-dimensional (2-D) Fourier transform of thekerneled AF.

By effective utilization of data interpolation and TF kernel, the proposed IA-MDR method achieves reliable IF estimation of all signal components, preserves a high resolution of auto-terms, improves energy concentration of the underlying TFDs, and provides robust TFDs by suppressing the undesired effects of cross-terms and artifacts. The proposed technique can be successfully applied to multi-component FM signals with large variations in their amplitude levels, and is particularly effective when a large number of data samples are missing as a result of either natural phenomenon, uneven sampling interval, or intentional under-sampling. The superiority of the proposed method is demonstrated through various simulation results.

Notations. A lower (upper) case bold letter represents a vector (matrix). $(\cdot)^T$, $(\cdot)^*$, and $(\cdot)^H$, respectively, define transpose, complex conjugation, and conjugate transpose (Hermitian). $\mathcal{F}_x(\cdot)$ and $\mathcal{F}_x^{-1}(\cdot)$, respectively, define the discrete Fourier transform (DFT) and inverse DFT (IDFT) with respect to x .

II. SIGNAL MODEL AND BI-LINEAR TIME-FREQUENCY DISTRIBUTIONS

A. Signal Model

Define a discrete-time K -component FM signal as

$$y(t) = \sum_{k=1}^K y_k(t), \quad t = 1, \dots, T, \quad (1)$$

where the k th signal component is given as

$$y_k(t) = A_k \exp(j\phi_k(t)), \quad t = 1, \dots, T, \quad (2)$$

where A_k and $\phi_k(t)$, respectively, represent the amplitude and time-varying angular phase of the k th signal component. The signal components are labeled according to their amplitude levels, from the highest to the lowest, i.e., $A_1 \geq \dots \geq A_K$.

Consider the observed data containing a total number of $M = \sum_{b=1}^B M_b$, $0 \leq M < T$, burst missing data samples with B being the total number of missing data bursts, and M_b denoting the number of missing samples in the b th burst. Missing data bursts are assumed to be mutually non-overlapping and their positions are randomly distributed over time. As such, the observed signal at the t th time instant, $r(t)$, can be expressed as the product of $y(t)$ and an observation mask, $R(t)$, i.e.,

$$r(t) = y(t) \cdot R(t), \quad (3)$$

where

$$R(t) = \begin{cases} 1, & \text{if } t \in \mathcal{S}, \\ 0, & \text{if } t \notin \mathcal{S}, \end{cases} \quad (4)$$

where $\mathcal{S} \subset \{1, \dots, T\}$ denotes the set of observed time instants and assumes a cardinality of $|\mathcal{S}| = T - M$.

It should be noted that a random missing sample scenario could be considered as a special case of the underlying burst missing sample scenario with $M_b = 1$ and $B = M$ in the above expressions.

B. Bi-linear Time-Frequency Distributions

The IAF of $r(t)$ is defined in the time-lag $(t-\tau)$ domain as

$$C_r(t, \tau) = r(t + \tau) r^*(t - \tau). \quad (5)$$

The WVD can be obtained by taking the 1-D DFT of the IAF with respect to τ as

$$W_r(t, f) = \mathcal{F}_\tau[C_r(t, \tau)] = \sum_{\tau} C_r(t, \tau) e^{-j4\pi f \tau}. \quad (6)$$

The ambiguity function (AF) is obtained by applying a 1-D DFT to the IAF with respect to time t , expressed as

$$A_r(\theta, \tau) = \mathcal{F}_t[C_r(t, \tau)] = \sum_t C_r(t, \tau) e^{-j2\pi \theta t}, \quad (7)$$

where θ is the frequency shift.

C. TF Kernels and Reduced Interference Distributions

Signal-adaptive TF kernels [11], [13] have been shown to be effective in mitigating undesired effects of cross-terms and missing data induced-artifacts from the respective TFDs. The radially Gaussian kernel function-based AOK [11] is one of the popular choices of such TF kernels. AOK is obtained by solving the following optimization problem for each time-localized, short-time ambiguity function (STAF):

$$\begin{aligned} & \max_{\Psi} \int_0^{2\pi} \int_0^{\infty} |A(\alpha, \varphi) \Psi(\alpha, \varphi)|^2 \alpha \, d\alpha \, d\varphi \\ & \text{subject to } \Psi(\alpha, \varphi) = \exp\left(-\frac{\alpha^2}{2\sigma^2(\varphi)}\right), \\ & \frac{1}{4\pi^2} \int_0^{2\pi} \sigma^2(\varphi) \, d\varphi \leq \beta, \end{aligned} \quad (8)$$

where $A(\alpha, \varphi)$ is the AF in the polar coordinate, $\Psi(\alpha, \varphi)$ is the Gaussian kernel function, $\sigma(\varphi)$ is the spread function that controls the spread of the Gaussian kernel at the radial angle $\varphi = \arctan(\tau/\theta)$, $\alpha = \sqrt{\theta^2 + \tau^2}$ is the radius, and parameter $\beta > 0$ trades off between the auto-component smearing and the cross-component suppression.

The time-localized TFD can be computed by taking the 2-D DFT of the corresponding kerneled AF, $\bar{A}(\alpha, \varphi) = A(\alpha, \varphi) \Psi_{\text{OPT}}(\alpha, \varphi)$. After converting the kerneled AF to the rectangular coordinate system, the corresponding RID is expressed as

$$D_{\text{AOK}}(t, f) = \mathcal{F}_{\theta}^{-1}\{\mathcal{F}_{\tau}[\bar{A}(\theta, \tau)]\}. \quad (9)$$

III. PROPOSED ITERATIVE ADAPTIVE MISSING DATA RECOVERY ALGORITHM

The proposed IA-MDR approach, developed for improved IF estimation of multi-component FM signals with missing data samples and distinct amplitude levels of the components, is described in this section.

A. Problem Formulation

We begin with the WVD, \mathbf{W}_r (6), as the underlying TFD. Let P be the total number of frequency grid points with f_p , $p = 1, \dots, P$, being the corresponding frequencies. At each time instant t , the column of \mathbf{W}_r defines the $P \times 1$ TF vector with sparsity K ($K \ll P$) and is denoted as $\mathbf{a}^{(t)}$, which is related to the corresponding $T \times 1$ IAF vector $\mathbf{b}^{(t)}$ as

$$\mathbf{b}^{(t)} = \mathbf{D}\mathbf{a}^{(t)}, \quad \forall t, \quad (10)$$

where \mathbf{D} is the $T \times P$ 1-D IDFT matrix. As all the operations in this section are performed at each time instant t , we omit superscript (t) from the expressions of $\mathbf{a}^{(t)}$ and $\mathbf{b}^{(t)}$ for notational simplicity.

The vector \mathbf{b} consists of two components: vector $\mathbf{b}_r = [b_{r_1}, b_{r_2}, \dots, b_{r_{Q_r}}]^T$ with Q_r measured IAF entries and vector $\mathbf{b}_m = [b_{m_1}, b_{m_2}, \dots, b_{m_{Q_m}}]^T$ with $Q_m = T - Q_r$ missing IAF entries. These two components are, respectively, given as

$$\mathbf{b}_r = \mathbf{\Gamma}_r \mathbf{b}, \quad \mathbf{b}_m = \mathbf{\Gamma}_m \mathbf{b}, \quad (11)$$

where the $Q_r \times T$ masking matrix $\mathbf{\Gamma}_r$ extracts the measured elements from vector \mathbf{b} , whereas the $Q_m \times T$ masking matrix

$\mathbf{\Gamma}_m$ extracts the missing elements. Similarly, the $Q_r \times P$ matrix $\mathbf{D}_r = \mathbf{\Gamma}_r \mathbf{D}$ and the $Q_m \times P$ matrix $\mathbf{D}_m = \mathbf{\Gamma}_m \mathbf{D}$, respectively, extract the rows of \mathbf{D} corresponding to the measured IAF entries in \mathbf{b}_r and the missing IAF entries in \mathbf{b}_m . Based on the measured data entries, Eq. (10) can be expressed as

$$\mathbf{b}_r = \mathbf{D}_r \mathbf{a}. \quad (12)$$

B. Proposed IA-MDR Algorithm

Each iteration of the proposed IA-MDR algorithm comprises of following three major steps:

- 1) Iterative adaptive amplitude spectrum estimation from the available data,
- 2) Missing data update, and
- 3) Application of signal adaptive TF kernel.

For each time instant t , the major steps of the proposed IA-MDR algorithm are summarized below.

We begin with the IAF vector of the available entries \mathbf{b}_r , the corresponding dictionary matrix \mathbf{D}_r , and the dictionary matrix corresponding to the missing IAF entries \mathbf{D}_m . The outer iteration counter, i , is set to 1. The TF vector at the t th time is initialized as $\mathbf{a}^{[0]} = \mathbf{a}$ obtained from (10).

Iterative amplitude spectrum estimation from the measured data:

Denote the complex-valued element of $\mathbf{a}^{[i-1]}$ corresponding to frequency f_p at the $[i; j]$ th iteration as $\alpha_p^{[i; j]}$, where j is the inner iteration counter. Let $S_p^{[i; j]} = |\alpha_p^{[i; j]}|^2$. Each column \mathbf{d}_{rp} of \mathbf{D}_r represents entries corresponding to frequency f_p . The covariance matrix of the available entries is obtained as

$$\mathbf{C}_r^{[i; j]} = \sum_{p=1}^P S_p^{[i; j]} \mathbf{d}_{rp} \mathbf{d}_{rp}^H. \quad (13)$$

The spectral amplitude corresponding to f_p is estimated as the solution to the weighted least squares criterion [20], [21],

$$\hat{\alpha}_p^{[i; j]} = \frac{\mathbf{d}_{rp}^H (\mathbf{C}_r^{[i; j]})^{-1} \mathbf{b}_r}{\mathbf{d}_{rp}^H (\mathbf{C}_r^{[i; j]})^{-1} \mathbf{d}_{rp}}. \quad (14)$$

The $\hat{\alpha}_p^{[i; j]}$ is iteratively updated until either the maximum number of iterations is reached or $|\hat{\alpha}_p^{[i; j]} - \hat{\alpha}_p^{[i; j-1]}|$ is less than a pre-defined threshold ϵ .

Missing data recovery and update:

Based on $S_p^{[i; j]}$ and the corresponding covariance matrices computed using (13), the missing IAF entries are recovered as follows [19]:

$$\hat{\mathbf{b}}_m^{[i; j]} = \sum_{p=1}^P S_p^{[i; j]} \mathbf{d}_{mp}^H (\mathbf{C}_r^{[i; j]})^{-1} \mathbf{b}_r \mathbf{d}_{mp}, \quad (15)$$

where \mathbf{d}_{mp} is the p th column of \mathbf{D}_m corresponding to frequency f_p .

The corresponding IAF vector $\hat{\mathbf{b}}^{[i; j]}$ is obtained as

$$\hat{\mathbf{b}}^{[i; j]} = \mathbf{\Gamma}_m^T (\mathbf{\Gamma}_m \mathbf{\Gamma}_m^T)^{-1} \hat{\mathbf{b}}_m^{[i; j]} + \mathbf{\Gamma}_r^T (\mathbf{\Gamma}_r \mathbf{\Gamma}_r^T)^{-1} \mathbf{b}_r. \quad (16)$$

Note that only the original missing entries of the IAF vector \mathbf{b} are updated with the corresponding entries of $\hat{\mathbf{b}}_m^{[i; j]}$, whereas \mathbf{b}_r remains unchanged.

Application of signal adaptive TF kernel:

Once the IAF vector $\hat{\mathbf{b}}^{[i;j]}$ is estimated, the corresponding AF is obtained by taking a 1-D DFT of the IAF with respect to time t using (7). Then, a signal adaptive TF kernel is applied to further improve the estimation and mitigate the effects of the cross-terms and missing data induced artifacts from the corresponding TFDs. In this paper, we have used AOK, however, any other signal adaptive TF kernel could be used in lieu of the AOK. The AOK for each time slice is computed using (8) and the corresponding reduced interference TFD, $\hat{\mathbf{a}}^{[i]}$ is obtained using (9). Then, the corresponding IAF vector $\mathbf{b}_{\text{AOK}}^{[i]}$ is obtained by taking a 1-D IDFT of $\hat{\mathbf{a}}^{[i]}$ with respect to frequency f . The original missing entries of the IAF vector \mathbf{b} are further updated with the corresponding entries of $\mathbf{b}_{\text{AOK}}^{[i]}$ as

$$\hat{\mathbf{b}}^{[i]} = \mathbf{\Gamma}_m^T (\mathbf{\Gamma}_m \mathbf{\Gamma}_m^T)^{-1} \mathbf{b}_{\text{AOK}}^{[i]} + \mathbf{\Gamma}_r^T (\mathbf{\Gamma}_r \mathbf{\Gamma}_r^T)^{-1} \mathbf{b}_r. \quad (17)$$

The iteration counter i is incremented by one and the entire procedure is repeated for either a pre-defined number of iterations or until the squared error between two subsequent signal estimates falls below a pre-defined threshold value, ξ , i.e.,

$$\|\hat{\mathbf{a}}^{[i]} - \hat{\mathbf{a}}^{[i-1]}\|_2^2 < \xi. \quad (18)$$

The final TFD is obtained by horizontally concatenating $\hat{\mathbf{a}}^{[i]}$ for all time instants, i.e.,

$$\mathbf{W}_{\text{IAMDR}} = [\hat{\mathbf{a}}_1^{[i]}, \dots, \hat{\mathbf{a}}_T^{[i]}]. \quad (19)$$

Note that in [22] the MIAA procedure described in (13)–(15) is applied only once. For multi-component signals, particularly when they have distinct amplitude levels, this approach does not provide sufficient capability to mitigate cross-terms and preserve weak signal components. The proposed approach overcomes this limitation by incorporating signal-adaptive TF kernels in the iterative loop, along with the application of MIAA in the IAF domain. The significant improvements, benefited from the data interpolation capability of the MIAA and the cross-term suppression capability of the signal-adaptive TF kernels, are clearly observed in the reconstructed TFDs. Besides, by only updating the original missing IAF entries in successive iterations while keeping the IAF entries associated with the observed signal unaltered, it ensures preservation of the distribution properties associated with the observed signal, and the reconstruction results are not adversely affected by the data filling operation of TF kernels.

IV. SIMULATION RESULTS

The proposed IA-MDR technique works well for both random as well as burst missing data sample scenarios. The effectiveness of the proposed method is demonstrated through various simulation results.

We consider a two-component FM signal with distinct amplitudes and closely separated signatures, given by

$$y(t) = \exp(j\phi_1(t)) + 0.4 \exp(j\phi_2(t)), \quad t = 1, \dots, T, \quad (20)$$

where $\phi_k(t)$ is the angular phase of the k th component at the t th time instant. T is chosen to be 128. The IF laws of these two components are respectively expressed as

$$\begin{aligned} f_1(t) &= 0.05 + 0.002t/T + 0.3t^2/T^2, \\ f_2(t) &= 0.15 + 0.006t/T + 0.24t^2/T^2. \end{aligned} \quad (21)$$

Figs. 1(a) and 1(b), respectively, show the real part of the original signal waveform without missing samples and the corresponding WVD. Due to the bi-linear nature of the underlying multi-component FM signal, the WVD exhibits severe cross-terms between components, even without missing samples.

First, we examine the performance of the proposed method in the presence of burst missing samples, and then, we investigate the random missing data scenario. In order to clearly demonstrate the effects of burst missing samples on the IF recovery performance, we first consider a noise-free case.

In the first scenario, we assume that the received signal contains a total of 48 (i.e., 37.5%) burst missing samples that are clustered into 12 groups, with each group containing 4 missing samples. The positions of these groups are randomly chosen, and are marked in red color in Fig. 2(a).

The comparison of the TFDs obtained using different methods is provided in Figs. 2(b)–2(g). The plot of true signal IFs is given in Fig. 2(h) for comparison purposes. The convolutive sinc-function-like artifact patterns, concentrated near the true IFs, are clearly visible in the WVD of Fig. 2(b). These strong artifact patterns make spectral estimation and analysis extremely challenging, and difficult to be suppressed using a signal adaptive TF kernel alone. While the AOK in Fig. 2(c) is successful in identifying stronger signal component, it provides erroneous result of the weaker signal component. In this scenario, the AOK optimization in the ambiguity domain may be misguided to favor such artifacts and generate an inaccurate detection of the signal components [8], in particular, the weaker ones. Figs. 2(d)–2(f), respectively, show the TFDs obtained from the application of the MIAA in the IAF domain [22], MISR applied to the kernelled IAF [8], and ALF-DTFD [24]. As seen from these figures, while these methods are generally successful in retrieving the stronger signal component, they either fail completely to recover weaker signal component or show excessive cross-terms and artifacts, hindering identification of true IFs of the weaker signal component. Note from Fig. 2(g) that the proposed IA-MDR approach successfully overcomes these limitations and achieves a precise estimation of true IFs of both signal components with high resolution, and also preserves distribution properties. Most of the cross-terms and artifacts are also effectively suppressed from the generated TFD of Fig. 2(g), with few non-significant exceptions at some places. The IA-MDR is applied for two iterations, where the AOK volume is chosen as 2.

In the second scenario, we assume that 50% of the data samples of the received signal are randomly missing, with their positions displayed in red color in Fig. 3(a). The signal-to-noise ratio (SNR) is chosen to be 15 dB. Unlike the previous burst missing data scenario, in the case of random missing samples, the artifacts are uniformly distributed in the entire TF region in their respective WVD of Fig 3(b).

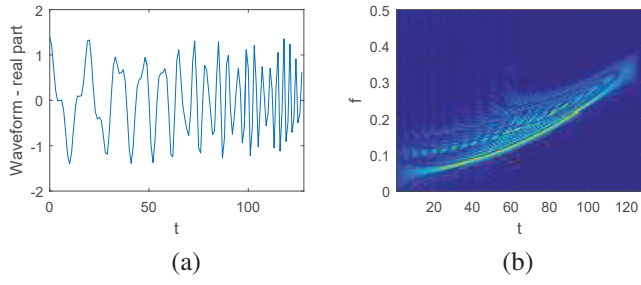


Fig. 1 The original signal without missing samples: (a) Real part; (b) WVD.

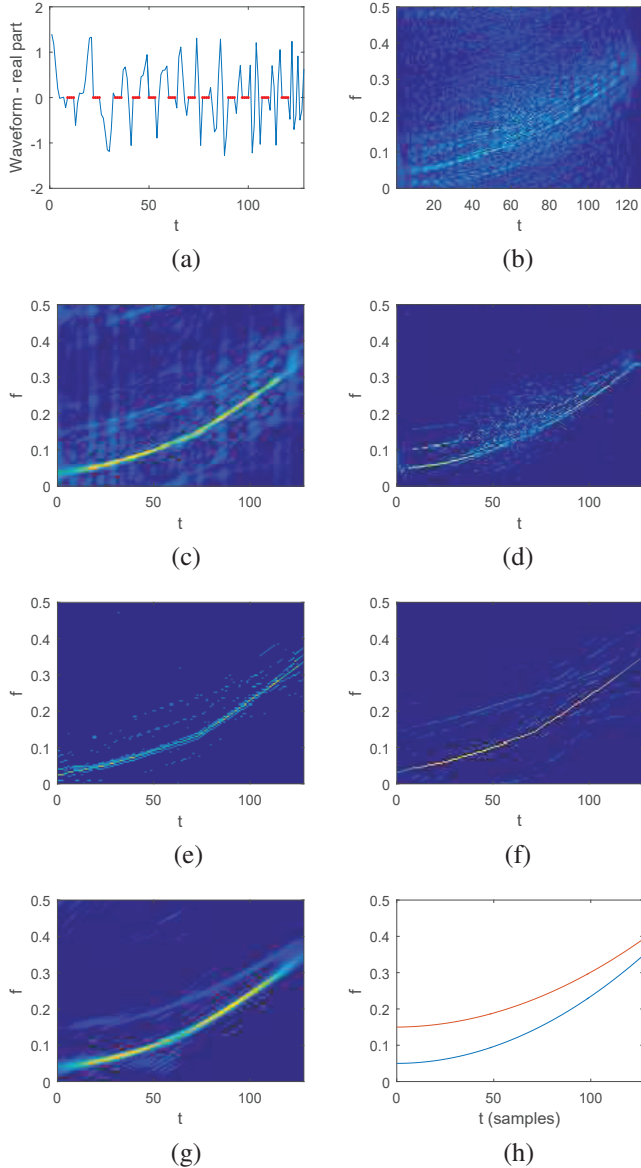


Fig. 2 TFDs obtained using application of different methods on the received signal containing 37.5% group missing data: (a) Real part of the received signal (with missing data positions marked in red color); (b) WVD; (c) AOK (volume 2); (d) MIAA applied to IAF; (e) MI-SR applied to the kernelled IAF; (f) ALF-DTFD; (g) Proposed IA-MDR; (h) True IFs (for comparison).

Along with the increased number of missing samples, the presence of noise makes it more difficult for the AOK of

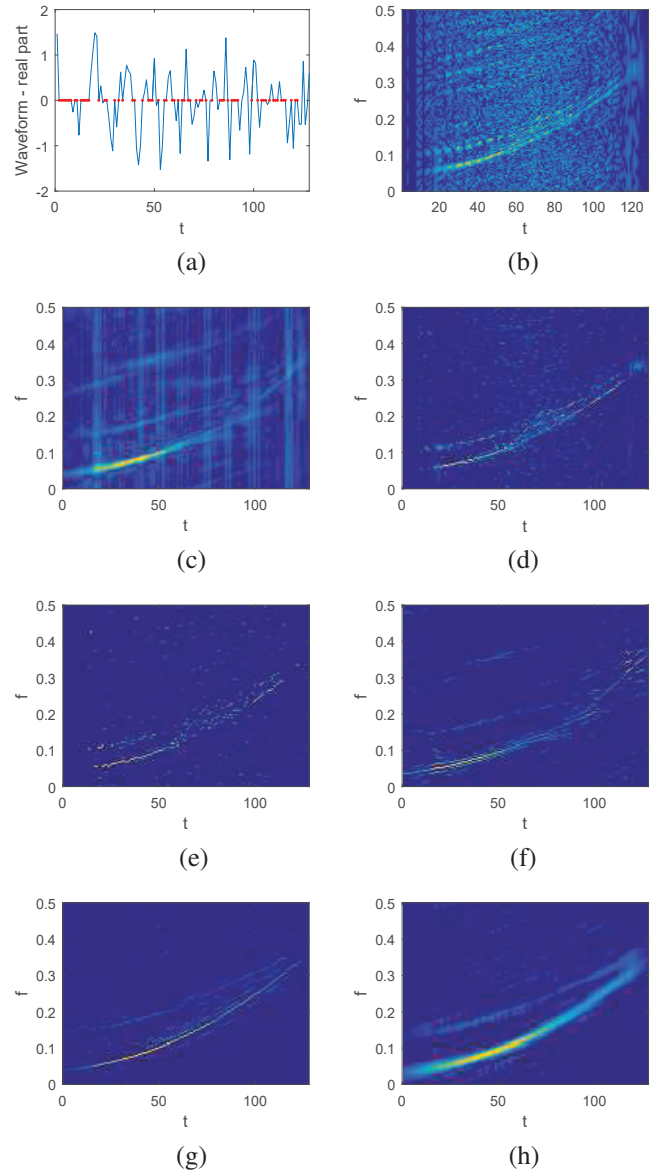


Fig. 3 TFDs obtained using application of different methods on the received signal containing 50% random missing data (SNR 15dB): (a) Real part of the received signal (with missing data positions marked in red color); (b) WVD; (c) AOK (volume 2); (d) MIAA applied to IAF; (e) MI-SR applied to the IAF of the received signal; (f) MI-SR applied to the kernelled IAF; (g) ALF-DTFD; (h) Proposed IA-MDR.

Fig. 3(c) to suppress the effects of noise and recover most of the weaker signal component. Figs. 3(d)-3(g), respectively, display the TFDs obtained using MIAA applied to the IAF, MI-SR directly applied to the signal IAF, MI-SR applied to the kernelled IAF, and ALF-DTFD. While the application of MIAA in the IAF domain is somewhat successful in retrieving the stronger signal component, the presence of strong artifacts misguides the identification of the weaker signal component and generates erroneous results. Besides, the scattered artifacts are clearly observed in the TF domain. In Fig. 3(e), the direct application of the MI-SR on the signal IAF generates similar results as Fig. 3(d) but achieves better cross-term and artifact mitigation. The application of the MI-SR on the IAF obtained from the AOK of Fig. 3(c) demonstrates better cross-

term and artifact suppression capabilities, and is successful in identifying some portions of the weaker signal component. The ALF-DTFD in Fig. 3(g) mitigates most of the cross-terms and artifacts, and also successfully identifies true IFs of most of the weaker signal component. However, it fails to preserve high energy of the weaker signal component. As seen in Fig. 3(h), the proposed IA-MDR algorithm achieves superior TF reconstruction results with an accurate estimation of the signal components, high energy concentration, and an effective cross-term and artifact mitigation. Three iterations of IA-MDR were applied with the associated AOK volume chosen to be 3.

Usually, 2 to 3 iterations of the IA-MDR method are sufficient to obtain the desired results, as most of the missing entries are updated during the first 2 to 3 iterations. Beyond that, only slight improvement is observed for each additional iteration.

V. CONCLUSIONS

In this paper, we have developed a new iterative approach that aims to recover missing IAF entries in conjunction with signal adaptive TF kernel, and thus, generates a robust TFD of multi-component FM signals in the presence of missing data samples. The proposed IA-MDR method provides an accurate IF estimation of the signal components, maintains high resolution of auto-terms, improves energy concentration of the underlying TFD, and also achieves an effective cross-term and artifact suppression, while preserving amplitude information of the signal components. When the FM signal has multiple closely separated components with large variations in their relative amplitudes, the proposed technique is found to be effective in resolving weaker signal components while maintaining high resolution of the true IFs, in contrast to some of the state-of-the-art techniques that fail to recover the weaker signal components.

REFERENCES

- [1] B. Boashash, "Estimating and interpreting the instantaneous frequency of a signal – Part 1: Fundamentals," *Proc. IEEE*, vol. 80, no. 4, pp. 520–538, Apr. 1992.
- [2] L. Cohen, *Time-Frequency Analysis: Theory and Applications*. Prentice-Hall, 1995.
- [3] V. Chen and H. Ling, *Time-Frequency Transforms for Radar Imaging and Signal Analysis*. Artech House, 2002.
- [4] P. Stoica, E. G. Larsson, and J. Li, "Adaptive filterbank approach to restoration and spectral analysis of gapped data," *Astron. J.*, vol. 120, pp. 2163–2173, Oct. 2000.
- [5] E. Larsson, G. Liu, P. Stoica, and J. Li, "High-resolution SAR imaging with angular diversity," *IEEE Trans. Aerosp. Electron. Syst.*, vol. 37, no. 4, pp. 1359–1372, Oct. 2001.
- [6] E. Larsson and J. Li, "Spectral analysis of periodically gapped data," *IEEE Trans. Aerosp. Electron. Syst.*, vol. 39, no. 3, pp. 1089–1097, July 2003.
- [7] Y. Wang, J. Li, and P. Stoica, *Spectral Analysis of Signals: The Missing Data Case*. Morgan and Claypool Publishers, 2006.
- [8] V. S. Amin, Y. D. Zhang, and B. Himed, "Sparsity-based time-frequency representation of FM signals with burst missing samples," *Signal Process.*, vol. 155, pp. 25–43, Feb. 2019.
- [9] B. Boashash, "Estimating and interpreting the instantaneous frequency of a signal – Part 2: Algorithms and applications," *Proc. IEEE*, vol. 80, no. 4, pp. 540–568, Apr. 1992.
- [10] L. Cohen, "Time-frequency distributions – A review," *Proc. IEEE*, vol. 77, no. 7, pp. 941–981, July 1989.
- [11] D. L. Jones and R. G. Baraniuk, "An adaptive optimal-kernel time-frequency representation," *IEEE Trans. Signal Process.*, vol. 43, no. 10, pp. 2361–2371, Oct. 1995.
- [12] B. Jokanovic, M. G. Amin, Y. D. Zhang, and F. Ahmad, "Time-frequency kernel design for sparse joint-variable signal representations," in *Proc. European Signal Process. Conf.*, Lisbon, Portugal, Sept. 2014.
- [13] N. Khan and B. Boashash, "Multi-component instantaneous frequency estimation using locally adaptive directional time frequency distributions," *Int. J. Adaptive Control Signal Process.*, vol. 30, pp. 429–442, Mar. 2016.
- [14] Y. D. Zhang, M. G. Amin, and B. Himed, "Reduced interference time-frequency representations and sparse reconstruction of undersampled data," in *Proc. European Signal Process. Conf.*, Marrakech, Morocco, Sept. 2013, pp. 1–5.
- [15] Q. Wu, Y. D. Zhang, and M. G. Amin, "Continuous structure based Bayesian compressive sensing for sparse reconstruction of time-frequency distributions," in *Proc. Int. Conf. Digital Signal Process.*, Hong Kong, China, Aug. 2014, pp. 831–836.
- [16] L. Stankovic, S. Stankovic, I. Orovic, and Y. D. Zhang, "Time-frequency analysis of micro-Doppler signals based on compressive sensing," in M. Amin (ed.), *Compressive Sensing for Urban Radars*, CRC Press, 2014.
- [17] M. G. Amin, B. Jokanovic, Y. D. Zhang, and F. Ahmad, "A sparsity-perspective to quadratic time-frequency distributions," *Digital Signal Process.*, vol. 46, pp. 175–190, Nov. 2015.
- [18] B. Jokanovic and M. G. Amin, "Reduced interference sparse time-frequency distributions for compressed observations," *IEEE Trans. Signal Process.*, vol. 63, no. 24, pp. 6698–6709, Dec. 2015.
- [19] P. Stoica, J. Li, and J. Ling, "Missing data recovery via a non-parametric iterative adaptive approach," *IEEE Signal Process. Lett.*, vol. 16, no. 4, pp. 241–244, Apr. 2009.
- [20] P. Stoica and R. L. Moses (Ed.), *Spectral Analysis of Signals*. Prentice-Hall, 2005.
- [21] T. Yardibi, J. Li, P. Stoica, M. Xue, and A. B. Baggeroer, "Source localization and sensing: A nonparametric iterative adaptive approach based on weighted least squares," *IEEE Trans. Aerosp. Electron. Syst.*, vol. 46, no. 1, pp. 425–443, Jan. 2010.
- [22] Y. D. Zhang, "Resilient quadratic time-frequency distribution for FM signals with gapped missing data," in *Proc. IEEE Radar Conf.*, Seattle, WA, May 2017, pp. 1765–1769.
- [23] J. A. Tropp and A. C. Gilbert, "Signal recovery from random measurements via orthogonal matching pursuit," *IEEE Trans. Inf. Theory*, vol. 53, no. 12, pp. 4655–4666, Dec. 2007.
- [24] V. S. Amin, Y. D. Zhang, and B. Himed, "Improved instantaneous frequency estimation of multi-component FM signals," in *Proc. IEEE Radar Conf.*, Boston, MA, Apr. 2019.
- [25] V. S. Amin, Y. D. Zhang, and B. Himed, "Sequential time-frequency signature estimation of multi-component FM signals," in *Proc. IEEE Asilomar Conf. Signals Syst. Comp.*, Pacific Grove, CA, Nov. 2019, pp. 1901–1905.
- [26] S. Zhang and Y. D. Zhang, "Robust time-frequency analysis of multiple FM signals with burst missing samples," *IEEE Signal Process. Lett.*, vol. 26, no. 8, pp. 1172–1176, June 2019.